International Journal of Modern Manufacturing Technologies
ISSN 2067–3604, Vol. XV, No. 2 / 2023
https://doi.org/ 10.54684/ijmmt.2023.15.2.127

MAGNETIC COMPOSITES FROM RECYCLED MATERIALS

Florin Stefan Mustata[1], Bogdan-Constantin Condurache[2], Antonela Curteza[1], Ciprian Ciofu[3], Stefan Grigorean[3]

[1] "Gheorghe Asachi" Technical University of Iasi-Romania, Faculty of Textiles and Industrial Management, Doctoral School, Blvd. Mangeron, No. 53, 700050, Iasi, Romania
[2] Laboratory of Inorganic Polymers, "P. Poni" Institute of Macromolecular Chemistry, Aleea Grigore Ghica Voda, No. 41 A, Iasi 700487, Romania
[3] "Gheorghe Asachi" Technical University of Iasi-Romania, Faculty of Mechanical Engineering, Blvd. Mangeron, No. 43, 700050, Iasi, Romania

Corresponding author: Florin St.C. Mustata, florinmustata@gmail.com

Abstract: In the conditions of the increasingly accentuated development of industrial and household products, the reuse of material waste with the aim of reducing environmental pollution has become an increasingly important necessity. This study presents the obtain of flexible magnetic composites based on cotton fabrics, acrylic rubber, powder from used tires and magnetite powder. The textile support was purchased from the local market (Tesatura Iași, Romania) and was made from 100% recovered cotton fibbers, with a mass of 143g·m^{-2} and an average thickness of 0.28mm. The rubber was an acrylate type (AR) (NipolR AR 51) with the next characteristics: (ρ = 1100Kg·cm^{-3} at 25ºC, Mooney viscosity ML (1+4) at 100ºC = 55; Tg = -4 ºC). The rubber powder (PW) (with more natural rubber in composition) was obtained by grinding at temperature under 10 ºC from used motorcycle tires obtained from the local market. The characteristic of rubber powder was: particles size up to 100 μm, moisture content < 0.25 %, density (ρ) = 1060 Kg·m^{-3}. Magnetite was obtained according to the literature [1]. The composites were obtained at the weight ratio of PW/AR/ (20/80) with added magnetite powder according to desired mass fraction. The materials and composites were characterized using infrared spectroscopy (FTIR), dynamic light scattering (DLS) technique, X-ray diffraction (WAXD), scanning electron microscopy (SEM) and vibrating sample magnetometer (VSM). These composites can be used as raw materials for smart materials in the high-tech applications in the production of the DC motors, recording apparatus, magnetic screens, radar technology, memory devices, magnetic and electromagnetic sensors, materials for medicine and environmental protection or in the electronic devices where flexibility is required.

Key words: acrylic rubber, used rubber powder, magnetite, magnetic composites

1. INTRODUCTION

Lately, flexible magnetic composites obtained from various polymers and magnetic materials in the form of powder have established themselves in the world of smart materials for the high-tech applications due to their specific properties (good elasticity and great flexibility) induced both by the polymer matrix and by the magnetic characteristics of the fillers [1-6]. Depending on the nature of the initial materials, the resulting composites in the form of flexible magnets present interesting physico-chemical and magnetic properties (vibration sensitivity, ability to absorb oscillations of different wavelengths, different deformations under the action of magnetic and mechanical forces, etc.). The large majority of these flexible composites use as matrices rubber-type polymers [1,3,5], epoxy or vinyl resins, biodegradable polymers such as polylactic acid, polycaprolactone, polysaccharides, etc. which in the initial phase are liquid products (by their nature or by dissolving or melting) which allows a more homogeneous dispersion of the magnetic powder [7-15]. This homogeneity gives good magnetic characteristics to the composites. This homogeneity gives good magnetic characteristics to the composites. These composites can be used in production of the DC motors, recording apparatus, magnetic screens, radar technology, biotechnology, surfaces with variable impedance, memory devices, inductive cores, magnetic and electromagnetic sensors, materials for medicine and environmental protection or in other electronic devices where flexibility is required.
Electromagnetic shielding as a phenomenon avoids interference problems between telecommunications devices and the environment in order to improve the efficiency of these devices. A mixture of conductive particles and magnetic particles dispersed in the polymer matrices can have a cumulative effect of blocking electrical and magnetic phenomena by the absorbing of the electric si and magnetic waves [16].

In this work, flexible magnetic composites were obtained using recycled cotton fabrics, acrylic rubber, powder from used tires and various amounts of magnetite powder.The main goal was to observe the influence of the amount of magnetite on the physical characteristics and to evaluate the magnetic properties of the prepared composites. The influence of magnetite on the morphological characteristics of the obtained products was also evaluated.

2. MATERIALS AND METHODS

2.1. Materials

The textile support was purchased from the local market (Tesatura, Iași, Romania) and was made from 100% recovered cotton fibbers. The fabric had a mass of 143 g m^{-2} and a average thickness of 0.28 mm.
The rubber (AR) was an acrylate type (NipolR AR 51) obtained from Nippon Zeon Co. Ltd. (Tokyo, Japan) with the next characteristics: (ρ = 1.1g cm^{-3} at 25 ^oC, Mooney viscosity ML (1+4) at 100^oC=55; Tg=-4^oC).
The rubber powder (with more natural rubber in composition) (PW) was obtained by manually physically processing (grinding) at room temperature (20^oC) from used motorcycle tires obtained from the local market (Iasi, Romania). The characteristic of PW was: particles size up to 100μm, moisture content < 0.25 %, density ρ=1060Kg/m^3.
Solvents, acetone (b.p.=56.5^oC, ρ=0.784g·cm^{-3}), ethyl acetate (b.p.=77.1^oC, ρ=0.902g·cm^{-3}) (Chemical Company, Iasi, Romania) and other chemicals (iron(II) sulfate heptahydrate ($FeSO_4$ x7H_2O, Sigma-Aldrich); ammonia solution 25% (NH_4OH 25%, Chemical Company,Iasi, Romania); hydrogen peroxide solution (H_2O_2 3%, Chemical Company, Iasi, Romania) with analytical purity were purchased from the local market and used as such. The materials used in the development of the present work were mainly of local origin, because the specific solution of local pollution problems and waste recovery in the region was pursued.

2.1.1. Obtaining of acrylic rubber solution (ARS)

The rubber solution was obtained by dissolving acrylic rubber under vigorous stirring at room temperature into solvent mixture (weight ratio of 75/25 g/g acetone/ethyl acetate) at weight ratio of solvent/AR of 84/16 g/g.

2.1.2. Synthesis of the Fe_3O_4 particles (PEPW)

Magnetite was obtained according to the modified literature using a partially modified recipe [22]. Thus, a 4-neck glass reactor with a capacity of 500ml was introduced into an electrically heated water bath, equipped with a mechanical stirrer, a descending condenser, a dropping funnel and a nitrogen supply source. In a first phase, in a vessel equipped as above, 20g of iron (II) sulfate heptahydrate ($FeSO_4$ x7H_2O) were dissolved under rapid stirring at room temperature in 200ml of distilled water. After filtering, the solution was stored in the first vessel. Then in the second vessel, 200ml of distilled water, 25.4ml of NH_4OH (25%) and 40 mL of H_2O_2 (3%) were introduced, which were homogenized at room temperature for 20 minutes. After the solution in the first vessel was heated to 80 °C under vigorous stirring, with the help of the dropping funnel, the second solution began to be added during one hour while maintaining the 80°C temperature. In a few minutes, black Fe_3O_4 particles appeared. After finishing the addition of the second solution, the temperature of the mixture was raised to 90°C, maintaining it at this temperature for another hour. The magnetite suspension was kept under stirring for 24 hours, after which it was sonicated, separated with the help of a strong magnet, filtered and washed several times with distilled water. To remove traces of water, several washes with ethyl alcohol were carried out. The drying was done at 25°C in a recirculation oven until constant weight.

2.1.3. Composite preparation

The rubber powder was added to the ARS at the weight ratio of PW/AR/ (20/80) and slowly stirred at room temperature for one day. Then the magnetite powder was added according to the desired mass fraction. After uniform mixing, the rubber composition was coated onto recycled textile fabric material to produce the flexible magnetic materials. The various thicknesses were obtained using an adjustable film applicator. The obtained composites were dried at room temperature in a recirculation oven until constant weight. From the composite prepared as above, the samples with different widths were extracted and used for the mechanical and magnetic measurements.

2.2. Methods

The dimension and the distribution of feritte particle were obtained by dynamic light scattering (DLS) technique with Zetasizer Nano-ZS apparatus (ZEN-3500-Malvern Instruments producer, Malvern, England) using a laser green light He-Ne (532 nm) at 173^oC and room temperature.

The aspect of the magnetic composites was studied using scanning electron microscopy technique (SEM), using a SEM/ESEM-Edax-Quanta 200 apparatus (FEI Company producer, Oregon,USA), equipped with a large field detector, at low vacuum (60-100)Pa and the acceleration voltage of 20KV. Fourier transform infrared (FT-IR) measurements were registered on a Vertex 70 apparatus (Bruker producer, Leipzig,Germany) in (400–4000)cm^{-1} domain with a resolution of 4cm^{-1}.The magnetite powder were blended with KBr, pressed as disks with a thickness of 0.3 up to 0.5 millimeters and the red FT-IR data were recorded. The FTIR spectra of magnetic composite samples were recorded registered using a MIRacle™ ATR accessory with diamond crystal plate with 1.8mm diameter. The obtained data, were processed with OPUS 6.5 software from Bruker, Germany.
The X-ray diffraction (XRD) observations of magnetite powder sample was recorded at room temperature by scanning with X–ray diffractometer with wide angle (in the range of $2\theta=20^o – 70^o$ diffraction angles (Bragg angle) using a Shimadzu LabX 6000 Diffractometer (Chiyoda-ku producer, Tokyo, Japan) using a CuK_α monochromatic radiation (λ = 0.1540568 nm), 36 kV and 25 mA.
The magnetic properties of magnetite and flexible composite materials were measured at 25ºC temperature with a vibrating sample magnetometer (VSM) of type Lake Shore model 8607 Lake Shore (Cryotronics producer, Inc., Westerville, USA). To avoid the vibration of the magnetite, the samples were mixed in molten bees wax and the mixtures were modelated in a spherical form with a mm diameter. Magnetic measurements were registere pe un interval de -30 to 30 kOe magnetic field. Initiallly each sample was demagnetized in alternating magnetic field.

3. RESULTS AND DISCUSSION

3.1. Characterization

3.1.1. Chemical characterization using FT-IR analysis

The chemical composition of the recycled fibers from which the fabric for composites is made was identified with the help of FT-IR analysis. In Figure 1 is shows the FT-IR spectrum and the signals values for each peak. The main peaks are situated near the following values: 3335, 2900, 1728, 1641, 1428, 1361, 1315, 1160, 1108, 1029, 896, 709 and 664 cm^{-1}. The strongest signals are located at 3.335 and at 2.900cm^{-1} and are attributable to the stretching vibrations of the hydroxyl and to CH, CH_2 groups. The adsorption band at 1.160 cm^{-1} is specific to the asymmetric bridge of C–O groups from hemicellulose, cellulose and lignin. The signal from 1.029 cm^{-1} is attributed to the bond C–O–C groups from the pyranose rings while the signals from the region 1.029–1.153 cm^{-1} are attributed to the C–H bonds. The linkages between glucose rings are present as a small peak at 896cm^{-1}. Additionally, the FT-IR spectra, can provide the information about the physical characteristics of the fibers. Thus, the signals from 1.428 cm^{-1} indicate if there is a crystalline area, while the signal from 896cm^{-1} indicate the amorphous zone.The chemical structures of AR and PW also were obtained using FT-IR analysis (Figure 2). In the IR spectra of AR, the specific signals for CH, CH_2, CH_3 groups are observed at 2954, 2926, and 2869cm^{-1} and can be coupled with the signals situated at 1463, 1380 and 1259cm^{-1}. The signals specific to the ester groups are located at 1725cm^{-1} for C=O groups and at 1167 and 1065cm^{-1} for asymmetric stretching vibrations of C-O-C groups. In the spectrum of rubber powde which is originally from the natural rubber, the signals located at 3323cm^{-1} can be assigned to OH groups and the signals located at 2915 and 2848cm^{-1} can be come from the vibration CH_2, CH_3 groups [23]. Also, CH_2, CH_3 groups can present signals and at 1426 and 1260cm^{-1}. The C = C double bond remaining after vulcanization can be present at 1635 and 951cm^{-1}. The signals for the composites with intermediate structure will be presented as a cumulaton between the signals of the two components.
The magnetite spectra were recorded with ATR (Bruker-Germany) modulus. FT-IR analysis was used to evidence the presence of maghemite–magnetite mixture in the chemical structure of the samples. Based of the literature data in the FT- IR spectra of magnetite (Figure 3a) the are few absorption signals located near 447, 572, and 635cm^{-1}. These signals can be atributed to the stretching and torsional vibration of Fe–O groups located in the structura de tip spinel a Fe_3O_4 [24, 25].
Also, the presence of adsorption band situated near 440cm^{-1} corresponds to the shifted of the Fe–O bond [19].The residual adsorbed water are located at 1631cm^{-1} and the residual hydroxyl groups vibration bands are located in the range of (3500-3400)cm^{-1} respectively at 3145 and 812cm^{-1}. The signals situated at 1132, 1058, and 981cm^{-1} can be assigned to a residual sulfate group which not totaly removed in the washing phase, [26].
In the case of composites (Figure 3b), the presence of magnetite not can be highlighted because the magnetite concentration is low (maximum 3%).

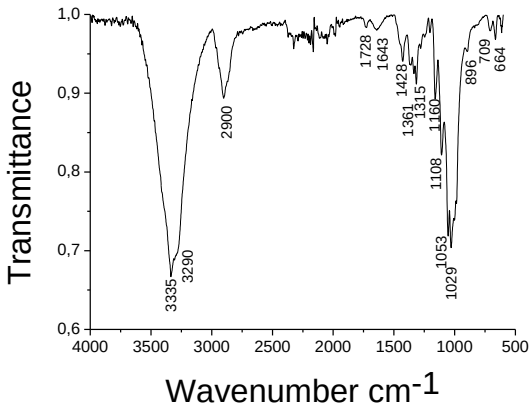

Fig.1. FT-IR for cotton

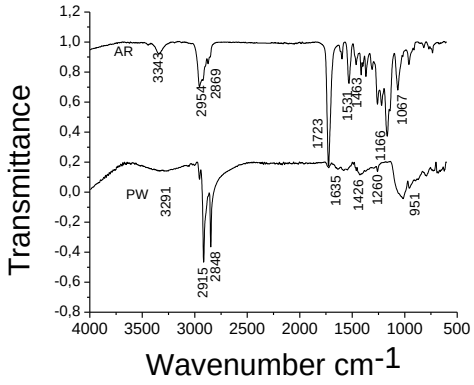

Fig. 2. FT-IR for AR and PW

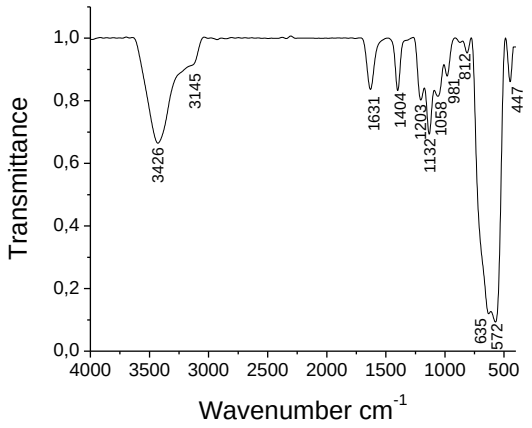

Fig. 3a. FT-IR for Fe_3O_4

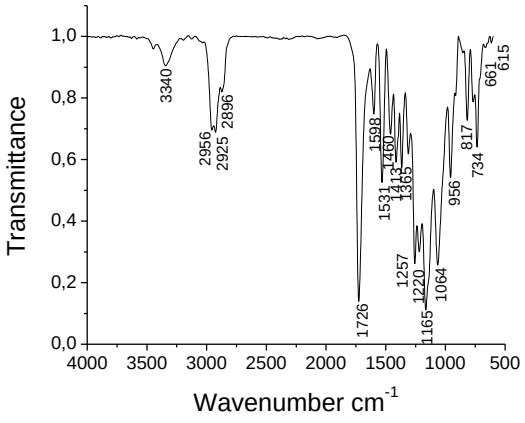

Fig. 3b. FT-IR for composite with 3% Fe_3O_4

3.1.2. Distribution of magnetite particle

The dimension and the distribution of feritte particle were obtained by dynamic light scattering (DLS) technique. The magnetite samples, with a concentration of 0.5% by mass, dispersed in deionized water with electrical conductivity of 0.06μS/cm, were ultrasonicated twice for 10 minutes, before measurement. The apparent hydrodynamic diameter of the sample was obtained using the Stokes-Einstein equation and was calculated as an average of 5 measurements. The hydrodynamic diameter of the magnetite sample is function of the mass and shape of the particles, the temperature, the ionic strength and the medium viscosity [27]. The size distribution registered at room temperature is presented in Figure 4. As seen in Figure 4, the distribution curve is having values between 200 and 1200nm with an average value of 373nm.

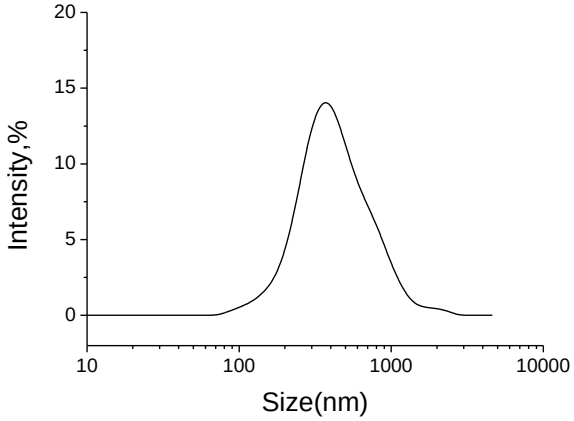

Fig. 4. The size distribution for Fe_3O_4 particles

3.1.3. X-ray characterization of magnetite

The results of X-ray analysis for the magnetite powders are shown in Figure 5 indicating showed mainly the presence of magnetite phase with a spinel type crystallinity with the peaks situated at 220, 311, 400, 422, 511 and 440 reflections. The weak diffuse scattering at small angles indicates the presence of a low amount of amorphous phase in the synthesized sample.The crystallne form is evidenced by strongest reflection situated at 220 and 311 plane. Using the XRD 311 peak registered data, the crystallite sizes calculated with Scherrer equation indicate a value of 16.7nm comparable with literature data. Also it can be observe a very good concordance between the registered data and literature (JCPDS file no: 19-0629) (Table 1), [28,29].

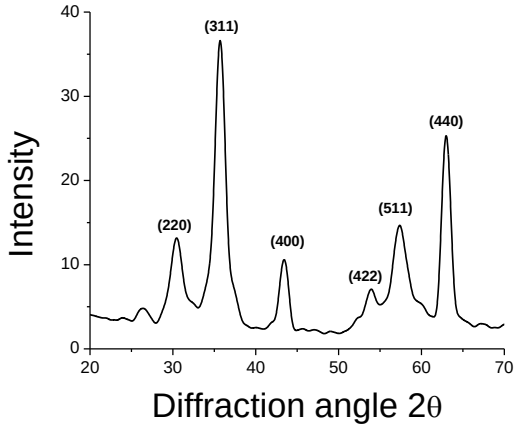

Fig.5. The X-ray peaks for Fe_3O_4 powder

Table 1. Comparison between measured data and literature data (JCPDS 00-019-0629) for (Fe_3O_4)

Sample	Peaks	File	Experimental data 2Θ	JCPDS 00-019-0629 2Θ
		JCPDS 00-019-0629		
Magnettite (Fe_3O_4)	220		30.14	30.05
	311		35.46	35.42
	400		43.06	43.05
	422		53.42	53.40
	511		57.00	56.94
	440		62.56	62.52

3.1.4. Morphological analysis of magnetite powder and composite

Scanning electron microscopy (SEM) was used to evaluate the composition and the appearance of the Unlike the composite with magnetite, the composite with iron in structure shown a relatively inhomogeneous aspect as a function of the Fe powder concentration. The SEM images show that the obtained magnetite generally consists of agglomerated particles with orthogonal shapes or sharp corners (Figure 6a). As can be seen in Figure 6b the flexible composite with magnetite in structure present a uniform surface of the polymeric materials, where the magnetite particles are distributed relatively homogeneous and uniform as a function of their concentration. Unlike the composite with magnetite, the composite with iron in structure shown a relatively inhomogeneous aspect asa function of the Fe powder concentration (Figure 6c). The data obtained with EDX module Quanta 200 device, for composite with magnetite in structure, highlighted the presence of magnetite from the iron ion.

3.1.5. Vibrating sample magnetometer (VSM)

Ferromagnetic and ferromagnetic materials, when subjected to the action of an external magnetic field, se magnetized. At low values of the external magnetic field, the magnetization phenomenon is reversible. The magnetization curves are recorded by measuring the magnetic induction values depending on the intensity of the magnetic field, thus obtaining the necessary information regarding the magnetic properties of the materials. By performing magnetic induction measurements in the increasing and decreasing direction of the magnetic field, a curve with hysteresis is obtained. The hysteresis curve provides data on saturation and reminisce induction, coercive and saturation fields, magnetic permeability etc., data that allow the evaluation of the usage characteristics of the tested materials. In the case of magnetic composites, their properties depend on the magnetic properties of the magnetite powder as well as the amount in which it is found in the structure of the composite. VSM magnetization curves for magnetite and flexible magnetic composites, at different magnetite content, are ilustrated in Figure 7abcdef. All the flexible magnetite composite samples and magnetite, present a similar magnetic behavior.

As can be seen from Figure 7abcdef, all the magnetization curves do not show the presence of a hysteresis loop, however, in the case of composites, very small deviations can be observed in the case of the images recorded by the device, this not being observable in the data made with the Origin graphics program. These deviations may be due to the fact that the magnetite nanoparticles are not perfectly dispersed in the polymer mass.
The very fine particles of crystalline magnetic material, as obtained in this work, do not show hysteresis curves and behave as super paramagnetic materials. As expected, due to the low concentrations of magnetite, the composites based on acrylic rubber, vulcanized rubber powder from used tires and magnetite powder, the magnetization does not show hysteresis and increases with the increase of the magnetic field [30,31].
The saturation magnetization for few concentrations in ferite are shown in Figure 7a,b,c,d,e,f Depending on the percentage of magnetite in the composite structure, the saturation magnetization increases from 1.025emu/g for the composites with 0.5% magnetite to 3.59 emu/g for the composites with 3% magnetite, having much lower values than the magnetization value for the initial magnetite (63.19emu/g). This is justified on the one hand by the shielding effect produced by the polymer composition as well as by the fact that the percentage of magnetite is very small. The values of the magnetic saturation depending on the concentration in the magnetite are presented in Table 2.

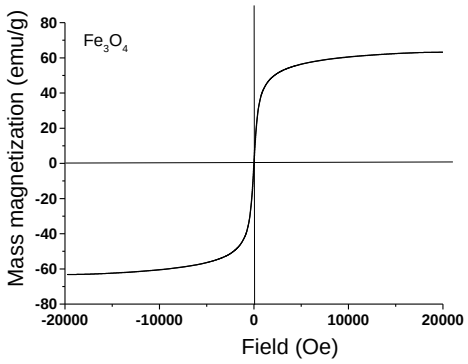

Fig.7a. The magnetization curves for 100% Fe_3O_4

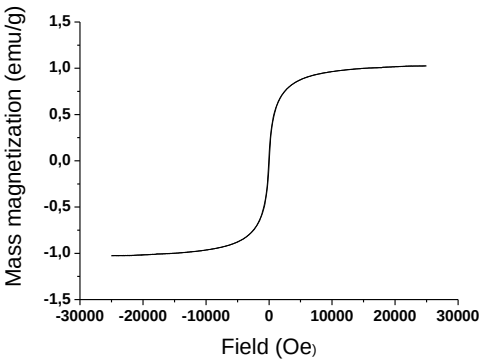

Fig.7b. The magnetization curves for flexible magnetic composition cotton/AR/PW with 0.5% Fe_3O_4

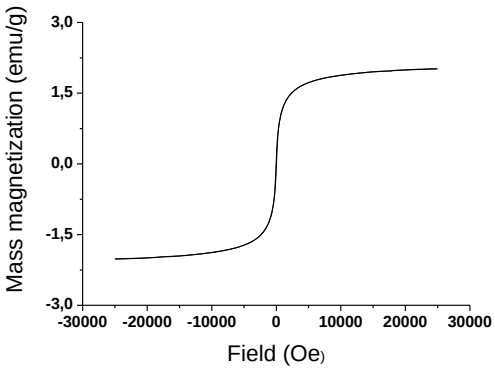

Fig.7c. The magnetization curves for flexible magnetic composition cotton/AR/PW with 1% Fe_3O_4

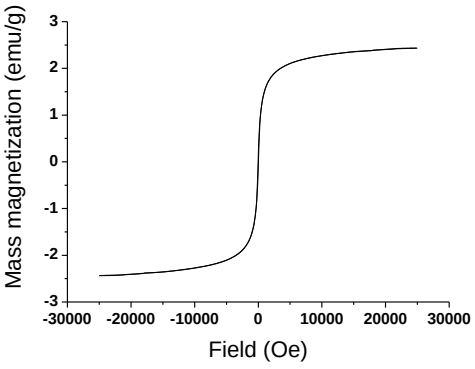

Fig.7d. The magnetization curves for flexible magnetic composition cotton/AR/PW with 1.5% Fe_3O_4

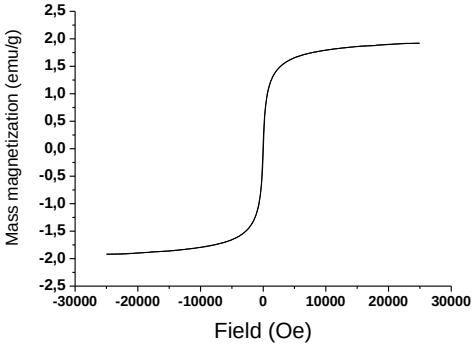

Fig.7e. The magnetization curves for flexible magnetic composition cotton/AR/PW with 2% Fe_3O_4

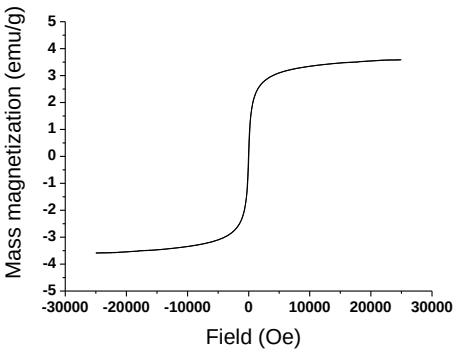

Fig.7f. The magnetization curves for flexible magnetic composition cotton/AR/PW with 3% Fe_3O_4

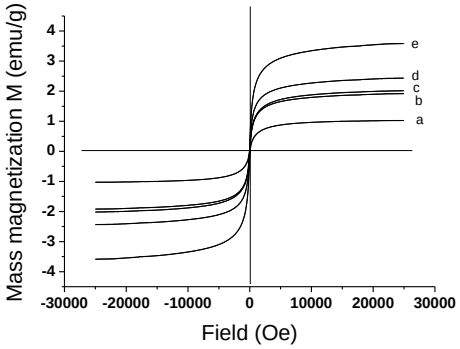

Fig.7. The magnetization curves for flexible magnetic composition cotton/AR/PW with: a- (0.5%), b- (1%),c -(1.5),d- (25), e- (3%) Fe_3O_4

Table 2. Saturation magnetization versus magnetite concentration

Sample	Magnetite concentration (%)	Saturation magnetization (emu/g)
Cotton/AR/PW/Fe_3O_4	0.5	1.925
Cotton/AR/PW/Fe_3O_4	1.0	2.011
Cotton/AR/PW/Fe_3O_4	1.5	2.021
Cotton/AR/PW/Fe_3O_4	2.0	2.432
Cotton/AR/PW/Fe_3O_4	3.0	3.591
Fe_3O_4	100	63.19

For comparison, flexible composites were obtained in which the magnetite powder was replaced with iron powder. The obtained results are presented in Figure 8 a, b, c, d, e, f and in Table 3.

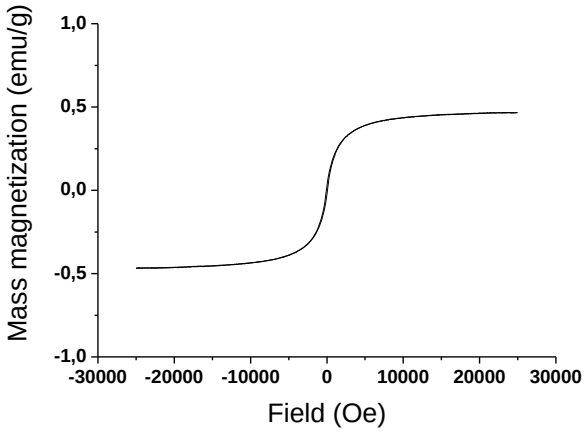

Fig.8a. The magnetization curves for flexible magnetic composition cotton/AR/PW with (7.5%) Fe.

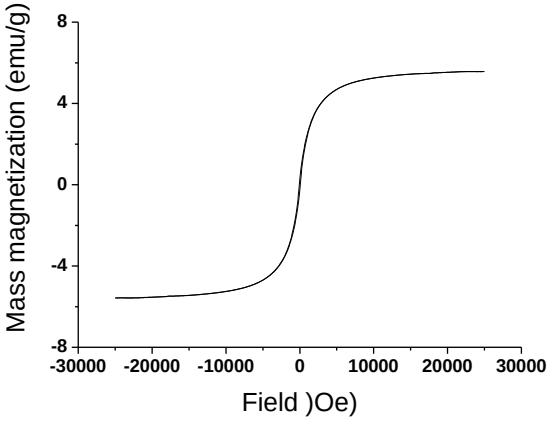

Fig.8b. The magnetization curves for flexible magnetic composition cotton/AR/PW with (19.0%) Fe.

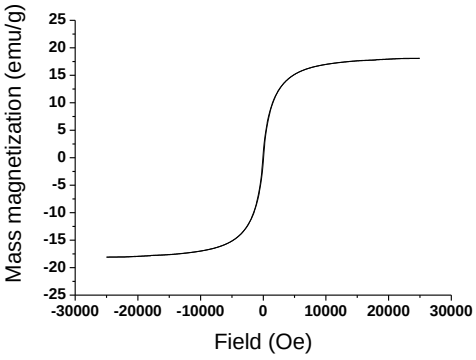

Fig.8c. The magnetization curves for flexible magnetic composition cotton/AR/PW with (28.0%) Fe.

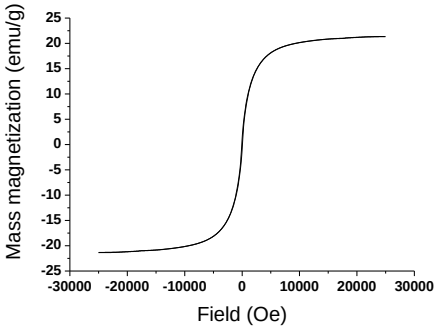

Fig.8d. The magnetization curves for flexible magnetic composition cotton/AR/PW with (37.5%) Fe.

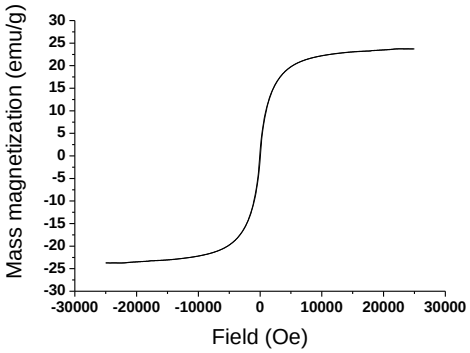

Fig.8e. The magnetization curves for flexible magnetic composition cotton/AR/PW with (45.0%) Fe.

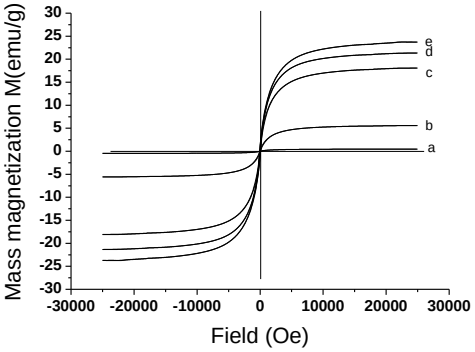

Fig.8. The magnetization curves for flexible magnetic composition cotton/AR/PW with: a- (7.5%), b-(19.0%), c -(28.0%), d-(37.5%), e -(45.0%) Fe.

Table 3. Saturation magnetization versus Fe concentration

Sample	Fe concentration (%)	Saturation magnetization (emu/g)
Cotton/AR/PW/Fe	7.5	0.50
Cotton/AR/PW/Fe	19.0	5.57
Cotton/AR/PW/Fe	28.0	18.08
Cotton/AR/PW/Fe	37.5	21.35
Cotton/AR/PW/Fe	45.0	23.71

4. CONCLUSIONS

This work confirms the preparation of a flexible magnetic composite by incorporation of magnetite powder, Fe powder in a polymer matrix from acrylic rubber and powder from used tires. Magnetite was obtained according to the literature using a partially modified recipe. The results of X-ray analysis for the feritte powders are shown in Figure 5 indicating showed mainly the presence of magnetite phase with a spinel type crystallinity with the peaks situated at 220, 311, 400, 422, 511 and 440 reflectionsThe physico-chemical characterization of magnetite and the other materials that make up flexible magnetic composites was done using were characterized by infrared spectroscopy (FT-IR), dynamic light scattering (DLS) technique, X-ray diffraction (WAXD), scanning electron microscopy (SEM) and vibrating sample magnetometer (VSM). The results of X-ray analysis for the magnetite powders showed mainly the presence of magnetite phase with a spinel type crystallinity with the peaks situated at 220, 311, 400, 422, 511 and 440 reflections. The incorporation of the magnetite powder in these flexible magnetic composite induced magnetic properties making them able to respond to the action of external magnetic fields. These methods confirmed the structure and highlighted the appearance and magnetic properties of magnetite and composites. These magnetic properties vary with the amount of magnetite from their structure. With the increase in the amount of magnetite, the magnetic properties of the composites also increase. Due to the low concentrations of magnetite, the composites based on acrylic rubber, vulcanized rubber powder from used tires and magnetite powder, the magnetization does not show hysteresis and increases with the increase of the magnetic field. The obtained composites from acrylic rubber as a polymer matrix and magnetite, on a textile support, are very flexible, have special mechanical resistance, allowing an easy incorporation into various electronic or mechanical devices, giving them good shielding properties. Although the amount of magnetite in the composite structure is small (up to 3%), the magnetic saturation has comparable values to that obtained with composites containing up to 20% Fe. This can be due both to the small size of the magnetite powder and to its relatively good dispersion in the entire mass of the composite.

REFERENCES

1.Soloman, M.A., Kurian, P., Anantharaman M.R., Joy, P.A., (2005). *Magnetic and processability studies of nitrile rubber vulcanisates containing barium magnetite and carbon black*. Indian J. Chem. Techn., 12, 582-587

2. Wang, Q., Yang, F., Yang, Q., Chen, J., Guan, H., (2010). *Study on mechanical properties of nano-Fe_3O_4 reinforced nitrile butadiene rubber.* Mater. Design.**,** 31, 1023–1028.

3. Guo, Z., Lei, K., Li,Y.,Ng., H.W., Prikhodko, S., Hahn, H.T., (2008). *Fabrication and characterization of iron oxide nanoparticles reinforced vinyl-ester resin nanocomposites.* Compos. Sci. Technol., 68 , 1513–1520.

4. Agarwal, K., Prasad, M., Sharma, R.B., Setua, D.K., (2011). *Studies on microstructural and thermophysical properties of polymer nanocomposite based on polyphenylene oxide and ferrimagnetic iron oxide*. Polym. Test., 30, 155-160.
5. El-Nashar, D.E., Ahmed, N.M., Agami, W.R., (2013). *The effect of new magnetite/kaolin pigment on the properties of acrylonitrile–butadiene rubber composites.* Mater. Design., 52, 108-117.
6. Souza, F.G., Ferreira, A.C., Varela, A., Oliveira, G.E., Machado, F., Pereira, E.D., Fernandes, E., Pinto, J.C., Nele, M., (2013). *Methodology for determination of magnetic force of polymeric nanocomposites.*Polym. Test., 32(8), 1466-1471.
7. Heidarian, P.; Kouzani, A.Z. (2023). *Starch-g-Acrylic Acid/Magnetic Nanochitin Self-Healing Ferrogels as Flexible Soft Strain Sensors.* Sensors, 23, 1138.
8. Cerdan, K.; Moya, C.; Van Puyvelde, P.; Bruylants, G.; Brancart, J. (2022). *Magnetic self-healing composites: Synthesis and applications.* Molecules, 27, 3796.
9. Hu, T.; Xuan, S.; Shu, Q.; Xu, Z.; Shen, L.; Li, J.; Gong, X. (2021). *Triple-shape memory, magneto-response, and piezo-resistive flexible composites: Multiple-sensing and switchable actuating.* J. Mater. Chem. C, 9, 6568–6578.
10. Calvo-Correas, T.; Shirole, A.; Crippa, F.; Fink, A.; Weder, C.; Corcuera, M.A.; Eceiza, A. (2019). *Biocompatible thermo-and magnetoresponsive shape-memory polyurethane bionanocomposites.* Mater. Sci. Eng. C, 97, 658–668.
11. Moghim, M.H.; Zebarjad, S.M.; Eqra, R. (2022). *Effect of Fe3O4 nanoparticles on magneto-responsive shape memory behavior of polyurethane-carbon nanotube nanocomposites*. J. Polym. Res., 29, 1–10.
12. Mudhar, R.; Mucolli, A.; Ford, J.; Lira, C.; Yazdani Nezhad, H. (2022). *Electrical and Magnetic Properties of 3D Printed Integrated Conductive Biodegradable Polymer Nanocomposites for Sustainable Electronics Development*. J. Compos. Sci., 6, 345.
13. De Souza, F., Marins, J., Pinto, J., de Oliveira, G., Rodrigues, C., Lima, L., (2010). *Magnetic field sensor based on a maghemite/polyaniline hybrid material*. J. Mater. Sci., 45, 5012-5021.
14. Souza Jr, F. G., Marins, J. A., Rodrigues, C. H. M., Pinto, J. C. A., (2010). *Magnetic Composite for Cleaning of Oil Spills on Water*. Macromol. Mater. Eng., 295, 942-948.
15. Lopes, M. C., Souza Jr, F. G., Oliveira, G. E., (2010). *Espumados magnetizáveis úteis em processos de recuperação ambiental.* Polímeros, 20, 359-365.
16. Prakash, V.A., Rajaduari, A., (2016). *Radio frequency shielding behavior of siline treated Fe_2O_3/E-glass fibre reinforced epoxy hybrid composite.* Appl. Phys., A 122, 875–883.
17. C. Ramesh, C., Prasanna, S.C., Maridurai, T., (2018). *Microwave shielding, dielectric and magnetic behaviour of mwcnt/fe3o4 pro-hybrid nano oxides reinforced natural rubber composite in E, F, I & J band frequencies.* Dig. J. Nanomat. Bio., 13 (4), 1103-1110.
18. Kruzelák, J., Sýkora, R., Dosoudil, R., Hudec, I., (2016). *Rubber Composites Based on Polar Elastomers with Incorporated Modified and Unmodified Magnetic Filler.* Hindawi Publishing Corporation, Advances in Materials Science and Engineering, Article ID 7242891
19. Hunyek, A., Sirisathitkul, C., Jantaratana, P., (2013). *Magnetic and dielectric properties of natural rubber and polyurethane composites filled with cobalt magnetite*. Plast., Rubber Compos., 42 (3), 89-92.
20. Jung, H.S., Kwon, S.H., Choi, H.J., Jung, J.H., Kim, Y.G., (2016*). Magnetic carbonyl iron/natural rubber composite elastomer and its magnetorheology.* Compos. Struct., 136 , 106–112.
21. Wu, J., Gong, X., Chen, I., Xia, H., Hu, Z., (2009). *Preparation and characterization of isotropic polyurethane magnetorheological elastomer through in situ polymerization*. J. Appl. Polym. Sci., 114, 901–910.
22. Condurache, B.-C., Cojocaru, C., Pascariu, P., Samoila, P., V. Harabagiu V., (2022). *Innovative nanostructured magnetite/wool/polysiloxane composite as magnetic adsorbent for oil spill removal*, CR. Chimie., 25(S3), 1-16.
23. Nallasamy, P., S. Mohan, S., (2004). *Vibrational spectra of cis-1.4-polyisoprene*, Arab. J. Sci. Eng., 29, 17-26.
24. Montagne, F., Monval-Mondain, O., Pichot, C., Mozzanega, H., Elaıssari, A., (2002). *Preparation and characterization of narrow sized (o/w) magnetic emulsion.* J. Magn. Magn. Mater., 250, 302–312.
25. Yamaura, M., Camilo, R.L., Sampaio, L.C., Macedom M.A., Nakamura, M., Toma, H.E., (2004). *Preparation and characterization of (3- aminopropyl)triethoxysilane-coated magnetite nanoparticles*. J. Magn. Magn. Mater., 279,:210–217. doi:10.1016/j.jmmm.2004.01.094
26. Fuentes-García, J. A., Carvalho Alavarse, A., Moreno Maldonado, A. C., Toro-Córdova, A., Ibarra, M. R., Goya, G.F., (2020). *Simple Sonochemical Method to Optimize the Heating Efficiency of Magnetic Nanoparticles for Magnetic Fluid Hyperthermia* ACS Omega, 5, 26357−26364.

21. Laurent, S., Forge, D., Port, M., Roch, A., Robic, C., Vander Elst, L., Muller, R.N., (2007). *Magnetic iron oxide nanoparticles: synthesis, stabilization, vectorization, physicochemical characterizations, and biological applications.* Chem Rev., 108:2064–110.
22. Reyes Villegas, V. A., De Leon Ramırez, J. I., Guevara, E. H., Perez Sicairos, S., Hurtado Ayala, L. A., Landeros Sanchez, B., (2020). *Synthesis and characterization of magnetite nanoparticles for photocatalysis of nitrobenzene,* J. Saudi Chem. Soc., 24, 223–235.
23. Lobato, N.C.C., Mansur, M.B., deM. Ferreira, A., (2017). *Characterization and chemical stability of hydrophilic and hydrophobic magnetic nanoparticles.* Mater. Res., 20, 736–746.
24. Mikhaylova, M., Kim, D.K., Bobrysheva, N., Osmolowsky, M., Semenov, V., Tsakalatos, T., Muhammed, M., (2004). *Superparamagnetism of magnetite nanoparticles: dependence on surface modification.* Langmuir, 20, 2472–2477.
25. B.D. Cullity, B.D., (1972). *Introduction to Magnetic Materials*, pp.411, Addison- Wesley, Reading, MA.

Received: July 17, 2023 / Accepted: December 15, 2023 / Paper available online: December 20, 2023 © International Journal of Modern Manufacturing Technologies